Specific problems in the CVD growth of graphene and carbon nanotubes

P. M. Rafailov[1*], V. B. Mehandzhiev[1], P. K. Sveshtarov[1], B. S. Blagoev[1], S. Sotirov[2],
S. Boyadjiev[1], V. Tomov[1], L. Yankova[1], D. Spassov[1], D. Z. Dimitrov[1,3]

[1]*Institute of Solid-State Physics, Bulgarian Academy of Sciences, 72, Tzarigradsko Chaussee Blvd., 1784 Sofia,
Bulgaria*
[2]*University of Plovdiv "Paisii Hilendarski", 24, Tsar Assen Str., 4000 Plovdiv, Bulgaria*
[3]*Institute of Optical Materials and Technologies, Bulgarian Academy of Sciences, Acad. G. Bonchev Str, Bl.109, 1113
Sofia, Bulgaria*

Graphene films were grown by chemical vapor deposition (CVD) on copper foils of varying thicknesses and on copper layers evaporated onto silicon plates. Plasma enhancement was applied during the CVD process to grow vertically aligned carbon nanotubes as well. The obtained specimens were characterized using micro-Raman spectroscopy, atomic force microscopy, and scanning electron microscopy. The relationship between the number of monolayers in the graphene films and the thickness of the copper catalyst substrate is discussed.

Keywords: Carbon nanotubes, Graphene, Chemical vapor deposition, Raman analysis

INTRODUCTION

A scalable growth method with good parameter control for graphene and related 2D heterostructures is the most important factor for the technological application of the unique properties of these novel materials. Chemical vapor deposition (CVD) has the potential to satisfy these requirements and is currently the dominant growth technique for "electronic-grade" large-area graphene films [1, 2]. Essentially, the CVD of graphene relies on a planar catalytic substrate, which aids the precursor dissociation and graphitic lattice formation at the high process temperatures and can host and maintain the graphene coating in the cooling stage and at ambient conditions [3]. Copper is established as a preferred substrate material because of its ability to form transient soft bonds at its surface facilitating the adsorption of C-species and, on the other hand, the widely assumed low solubility of carbon in copper. [4].

In order to obtain high-quality monolayer graphene containing large single-crystalline grains, the graphene nucleation density in the growth stage must be kept sufficiently low. Although various surface pretreatment methods like electropolishing help decreasing the nucleation density [5], it was recently shown that the decisive factor for its uncontrollable increase during the CVD process is the amorphous/graphitic carbon trapped beyond the thermodynamic solubility in the bulk and the (sub-) surface regions of the copper foil [6] during its production, e.g. along the rolling striations.

Thus, even after a thorough surface pretreatment, failing to deactivate this deleterious carbon may lead to higher nucleation density and possibly to formation of bi- or few-layer graphene regions.

CVD is also one of the most efficient techniques for growth of carbon nanotubes (CNTs) provided suitable catalyst nanoparticles are present [7]. The precursor dissociates at the surface of the catalyst nanoparticle supplying the carbon species needed for nanotube growth. The catalyst particle may get attached either on top (top-growth mode) or stay at the bottom of the nanotube (base-growth mode) [8]. An important advantage of the CVD method is that it allows control over the nanotube morphology and can produce more or less aligned CNTs. However, scalability to large–volume production and reproducibility still remain a challenge for the nanotube CVD [9].

For additional confirmation of the role of the Cu-foil carbon content in the graphene growth process we carried out a typical CVD recipe for single-layer graphene with Cu substrates of different thickness and report the results in this communication. We also report results on plasma-enhanced CVD growth of carbon nanotubes.

EXPERIMENTAL

Graphene and carbon nanotubes were grown by CVD in a cold-wall Plasmalab System 100 research reactor from Oxford Instruments. According to the established recipe for monolayer graphene (MLG) growth [10] the substrate was first heated to 1065 °C

---

* To whom all correspondence should be sent:
E-mail: *rafailov@issp.bas.bg*

in an Ar and H_2 flow, with flow rates of 1500 and 150 sccm, respectively, for 30 minutes of annealing. Subsequently, a flow of 10 sccm CH_4 combined with 50 sccm H_2 flow, were introduced into the reaction chamber for 30 minutes for the growth stage. At the end of the process, the sample was quenched to 300 °C at a rate of 15 °C /min in hydrogen/argon atmosphere and then cooled to room temperature in pure Ar.

Carbon nanotubes were grown from acetylene gas precursor in a mix of Ar and H_2 as carrier gases and NH_3 as additional radical source (gas purity 99.999 %) in the temperature range 800–950 °C. The substrates were semiconductor silicon wafers coated with TiN diffusion barrier and 5 nm Ni catalyst film. Capacitively coupled radio-frequency (RF) (13.56 MHz) plasma was ignited in the chamber during both the pretreatment and growth steps. The 5 nm Ni film was activated by the plasma at the growth temperature during the predeposition step and turned into catalyst nanoparticles.

The Raman spectra were measured in backscattering geometry using HORIBA Jobin Yvon Labram HR visible spectrometer equipped with a Peltier-cooled charge-coupled device (CCD) detector. The 633-nm line of a He-Ne-laser was used for excitation. The laser beam was focused on spots of different size using microscope optics.

The AFM images were obtained with a Nanosurf FlexAFM atomic force microscope, using the tapping mode. The AFM microscope is equipped with a silicon AFM probe for operation in non-contact and tapping mode TAP 190 Al-G.

RESULTS AND DISCUSSION

I. Graphene

As most of the graphene growth experiments so far have been conducted on standard 25 μm thick copper foils, it would be interesting to compare the results of the same recipe carried out on Cu substrates of different thickness. Initially, it was believed that graphene growth takes place in self-limited adsorption-driven mode [4]. However, recent reports on bilayer graphene (BLG) synthesis demonstrated that such CVD growth may not be self-limited for processes at ambient pressure [11]. Therefore, for our experiments we chose a low-pressure growth (4000 mTorr) mode in order to rule out atmospheric pressure as a factor facilitating formation of thicker-than-monolayer graphene. A standard 25 μm thick copper foil and another foil with 125 μm thickness were used as substrates and were subjected to the same pretreatment procedure including electropolishing. Additionally, graphene was also deposited on a 500 nm thick Cu layer evaporated on a standard SiO_2/Si plate.

Figure 1 shows an AFM image and a height profile that are representative for the surfaces of the samples of both thicknesses after the graphene growth. Although the surfaces are relatively rough compared to the atomic thinness of the graphene, characterization usually reveals almost full graphene coverage as graphene compensates this roughness with increased formation of wrinkles and tears [12]. Furthermore, the lateral grain dimensions of the Cu surface do not limit the size of graphene domains which can easily overgrow their boundaries [13].

(a)	(b)
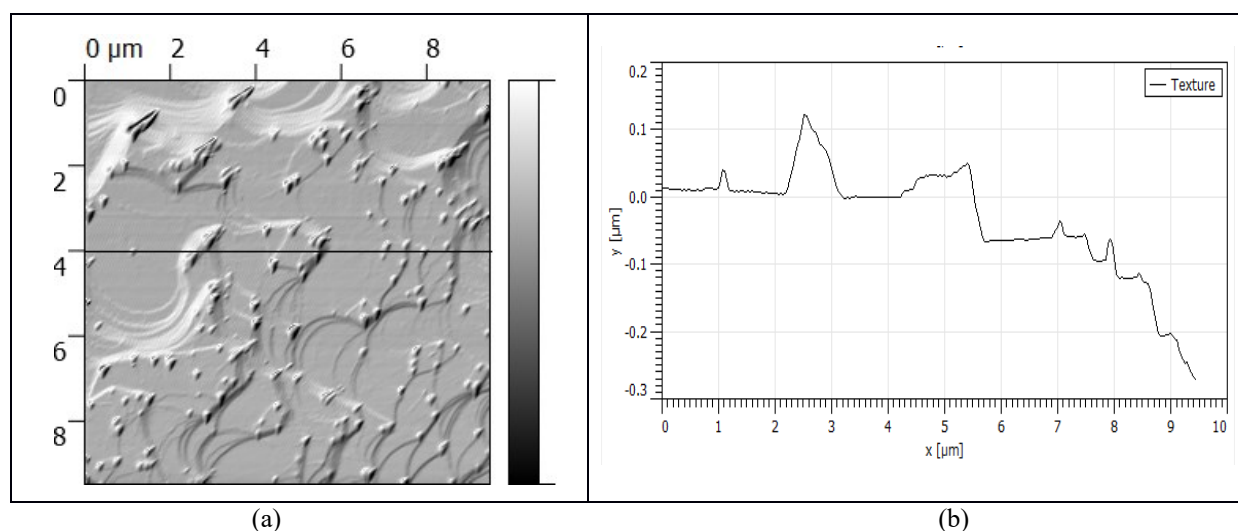
Figure 1. (a) AFM image of Cu foil substrate after graphene growth process. (b) Height profile recorded along the horizontal line in panel (a).

Thin   Thick   (a)

(b)
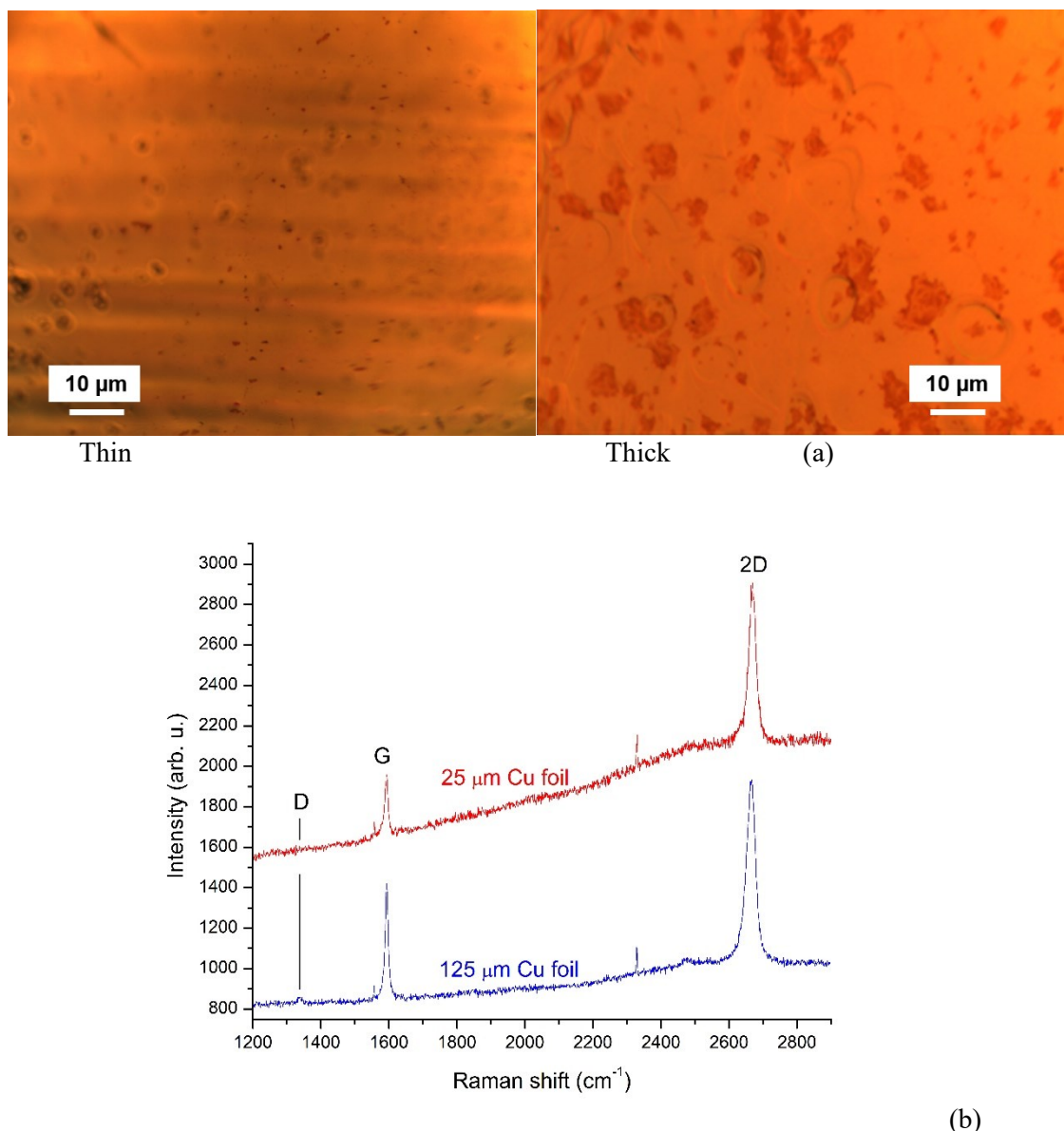
Figure 2. (a) Optical micrographs from the thick and thin Cu foil substrates. (b) Representative Raman spectra from these specimens.

Table 1. Raman spectral parameters of graphene samples.

Graphene sample on:	Band positions, cm^{-1}		Peak intensity ratio I(2D)/I(G)	2D band width, cm^{-1}
	G	2D		
25 μm Cu foil	1593	2665	2.7	26
125 μm Cu foil	1593	2667	1.5	30
500 nm Cu layer on Si	1592	2665	2.2	36
Free-standing MLG (reference)	1585	1630	3	25 - 30

To test the deposited graphene coating, Raman spectra were recorded from several points of the CVD processed copper substrates of different thickness. A full graphene coverage of the copper substrate was established. Figure 2(a) shows microscopic images of the copper foils taken several days after the graphene deposition. The samples exhibit mainly orange color indicating blank copper with occasional small spots of pale-red (or rosa) color indicating slight copper oxidation (Cu_2O) which slowly develops beneath the graphene coating [10]. Figure 2(b) depicts typical Raman spectra from the nonoxidized (blank copper) areas. Some important numerical results from these Raman

spectra are summarized in Table 1 along with reference data.

As can be seen from Table 1, the Raman examination finds upshifted graphene bands with low-intensity, which is characteristic of strong graphene coupling to the Cu substrate [14]. The peak intensity ratio I(2D)/I(G) of the 2D and G bands, which is indicative of the number of monoatomic layers in a graphene film [15] is ≈ 2.7 for the graphene grown on the 25 μm foil and ≈ 1.5 for that grown on the 125 μm foil. Although I(2D)/I(G) may be compromised by the graphene-Cu coupling which impacts the intensity of G and 2D band in different ways, these two sharply different values undoubtedly indicate predominantly MLG on the 25 μm foil and a significant presence of BLG on the thicker foil. On the other hand, the examined graphene coatings appear to be of good quality as can be appreciated from the faint D band intensity and the 2D bandwidth which is around 30 cm^{-1} for all spectra, i.e. it is not significantly broadened [15]. The Raman characterization thus reveals that a CVD growth recipe, which leads to MLG formation in the standard case, forms BLG on significantly thicker copper foil. Figures 3(a) and 3(b) show Raman spectra from the Cu layer on Si plate after the graphene growth process and an optical micrograph of the specimen, respectively. We conclude that during the CVD process on the thicker Cu foil there is an oversupply of carbon species from its sub-surface regions which leads to enhanced formation of bilayer graphene. This confirms the arguments raised in Ref. [6] for the importance of effectively controlling the carbon content of the Cu substrate for graphene CVD. On the other hand, the thin Cu film on SiO$_2$/Si coagulates into droplet-like structures which are overgrown with monolayer graphene. However, the bare SiO$_2$/Si surface, which emerges from this dewetting process, is not coated with graphene.

(a)   (b)
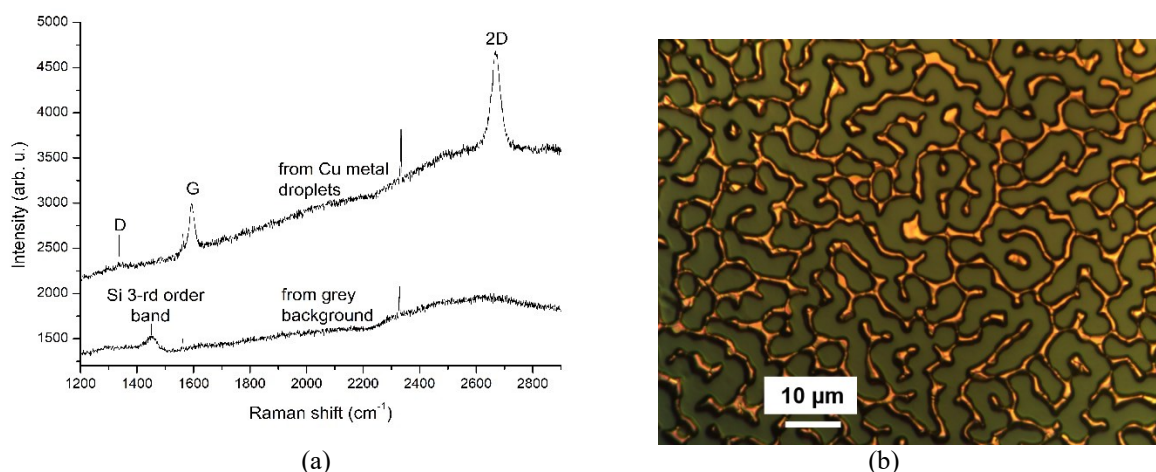
Figure 3. (a) Raman spectra of graphene grown on thin Cu layer evaporated on SiO$_2$/Si. (b) Optical micrograph from the specimen after the graphene growth process.
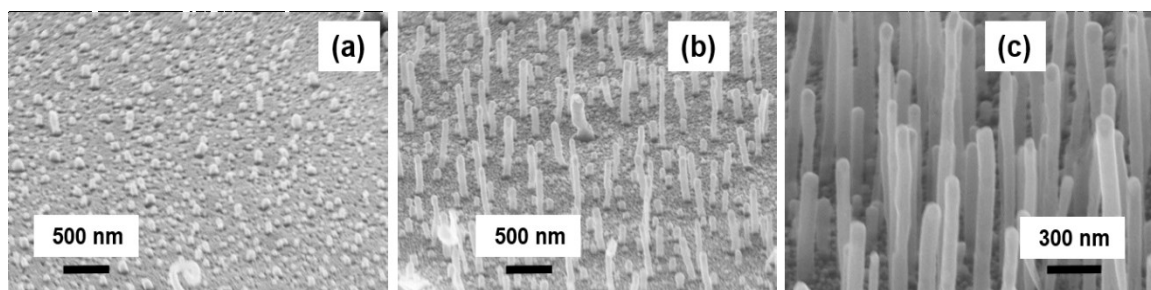
Figure 4. SEM micrographs from different stages of the CNT growth process. (a) activated catalyst seeds; (b) growing nanotubes with varied length; (c) straight well aligned CNT array.

II. Carbon nanotubes

In the present experiments, a Ni/TiN/Si substrate was used. The growth of carbon nanotubes at a reasonable rate requires plasma activation of the reacting species. The thin top Ni layer is decomposed into small nanoparticles in the pre–growth step by electron bombardment in NH_3+H_2 plasma, thus providing the catalyst centers for the growth start. Growth takes place *via* carbon species adsorption and trapping at atomic steps at the Ni nanoparticles' surface. It is facilitated by cyano–containing radicals from the ammonia which combine with acetylene–derived species in the plasma [16]. The presence of the intermediate TiN layer favors tip-growth mode [17, 18] which was indeed observed in the present case, the nanotube diameter being to a large extent defined by the catalytic nanoparticle. The RF electric field provides orienting force that facilitates the formation of straight nanotubes aligned perpendicular to the substrate.

Figure 4 displays SEM micrographs of the obtained CNTs in different stages of their growth. They are identified as multi-walled tubes with average diameter of ≈ 80 nm and length of about 1 - 2 μm. Figure 5 shows representative Raman spectra from these objects. The spectra display the typical Raman features of multiwalled CNTs. Multiwalled nanotubes typically contain a lot of incommensurate structures and CVD grown CNTs exhibit a high content of impurities, such as graphitic compounds, amorphous carbon, unreacted metal particles etc. The intense and broadened D/G band doublet points to a considerable amount of amorphous carbon. High temperature heat treatment in an oxidizing atmosphere [19] is typically used to remove the amorphous and disordered graphitic phases.
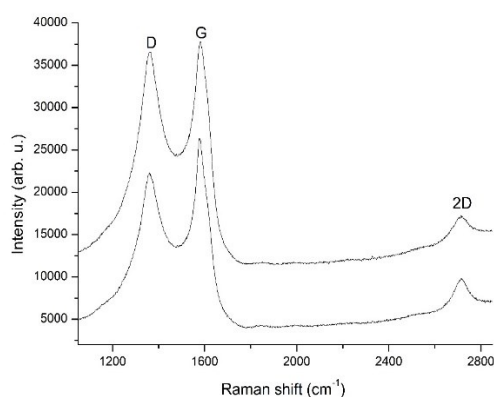
Figure 5. Representative Raman spectra from the obtained carbon nanotube arrays.

CONCLUSIONS

Graphene films were grown by chemical vapor deposition (CVD) on Cu foils of different thicknesses and Cu-layer coated Si plate and characterized by micro-Raman spectroscopy, optical and atomic force microscopy. Raman characterization reveals graphene with low defect density and good homogeneity. However, on the thicker (125 μm) Cu foil there was an increased formation of bilayer graphene. We attribute the formation of thicker graphene to the oversupply of carbon species from the bulk and (sub-)surface regions of the thicker Cu foil during the growth process. Additionally, vertically aligned carbon nanotubes, perpendicular to the substrate, were grown by plasma-enhanced CVD and confirmed with Raman spectroscopy and scanning electron microscopy.

REFERENCES

1. X. Li, W. Cai, J. An, S. Kim, J. Nah, D. Yang, R. Piner, A. Velamakanni, I. Jung, E. Tutuc, S. K. Banerjee, L. Colombo, R. S. Ruoff, *Science*, **324**, 1312 (2009).
2. Z. Yan, Y. Liu, L. Ju, Z. Peng, J. Lin, G. Wang, H. Zhou, C. Xiang, E. L. G. Samuel, C. Kittrell, V. I. Artyukhov, F. Wang, B. I. Yakobson, J. M. Tour, *Angew. Chem. Int. Edn.*, **53**, 1565 (2014).
3. S. Hofmann, P. Braeuninger-Weimer, R. S. Weatherup, *J. Phys. Chem. Lett.*, **6**, 2714 (2015).
4. R. Muñoz, C. Gómez-Aleixandre, *Chemical Vapor Deposition*, **19**, 297 (2013).
5. M. Griep, E. Sandoz-Rosado, T. Tumlin, E. Wetzel, *Nano Lett.*, **16**, 1657 (2016).
6. P. Braeuninger-Weimer, B. Brennan, A. J. Pollard, S. Hofmann, *Chem. Mater.*, **28**, 8905 (2016).
7. M. Meyyappan, L. Delzeit, A. Cassell, D. Hash, *Plasma Sources Sci. Technol.*, **12**, 205 (2003).
8. M. Kumar, Y. Ando, *J. Nanosci. Nanotechnol.*, **10**, 3739-3758 (2010).
9. K. B. K. Teo, C. Singh, M. Chhowalla, W. I. Milne, Catalytic Synthesis of Carbon Nanotubes and Nanofibers, in: Encyclopedia of Nanoscience and Nanotechnology, volume **X**, H. S. Nalwa (ed.) American Scientific Publishers, 2003, p. 1.
10. P. M. Rafailov, P. K. Sveshtarov, V. B. Mehandzhiev, I. Avramova, P. Terziyska, M. Petrov, B. Katranchev, H. Naradikian, S. I. Boyadjiev, C. Cserháti, Z. Erdélyi, I. M. Szilágyi, *Molecules*, **27**, 1789 (2022).

11. P. Trinsoutrot, C. Rabot, H. Vergnes, A. Delamoreanu, A. Zenasni, B. Caussat, *Surf. Coat. Technol.*, **230**, 87, (2013).

12. J.-Y. Hong, Y. C. Shin, A. Zubair, Y. Mao, T. Palacios, M. S. Dresselhaus, S. H. Kim, J. Kong, *Adv. Mater.*, **28**, 2382 (2016).

13. V. L. Nguyen, Y. H. Lee, *Small*, **11**, 3512 (2015).

14. E. Cazzanelli, O. de Luca, D. Vuono, A. Policicchio, M. Castriota, G. Desiderio, M. P. de Santo, A. Aloise, A. Fasanella, T. Rugiero, R. G. Agostino, *Journal of Raman Spectroscopy*, **49**, 1006 (2018).

15. A. C. Ferrari, J. C. Meyer, V. Scardaci, C. Casiraghi, M. Lazzeri, F. Mauri, S. Piscanec, D. Jiang, K. S. Novoselov, S. Roth, A. K. Geim, *Phys. Rev. Lett.*, **97**, 187401 (2006).

16. M. S. Bell, K. B. K. Teo, R. G. Lacerda, W. I. Milne, D. B. Hash, M. Meyyappan, *Pure Appl. Chem.*, **78**, 1117 (2006).

17. A. Gohier, T. M. Minea, M. A. Djouadi, J. Jiménez, A. Granier, *Physica E*, **37**, 34 (2007).

18. A. Gohier, C. P. Ewels, T. M. Minea, M. A. Djouadi, *Carbon*, **56**, 1331 (2008).

19. M. Endo, T. Hayashi, Y. A. Kim, H. Muramatsu, *Jpn. J. Appl. Phys.*, **45**, 4883 (2006).